

図2 Drexler らの記録した functional OCT 画像

- a : 網膜断層像の白黒イメージを左端に示し、対応する functional OCT 信号の時間的経過を疑似カラーで示す。左カラー図は刺激なし、中央は通常の1発フラッシュ、右は視細胞を薬物で抑制した状態の1発フラッシュによる信号を示している（以下同様に配列）。赤破線に囲まれた部分が視細胞層に相当する。中央の1発フラッシュに注目すると、視細胞外節に相当する部位の反射率が若干上昇している。
- b, c : a の画像を反射率の上昇 (b) と低下 (c) に分けて3次元的に表したもの。赤破線で囲まれた部分が視細胞層に相当する。中央の1発フラッシュに注目すると、視細胞内節の反射率は低下し、外節の反射率は上昇している。
- d, e : 視細胞内節 (d) および外節 (e) に相当する部位の信号強度を時間経過で表したもの。黄色いラインはフラッシュ刺激を示す。中央の1発フラッシュでは、刺激後に反射率が低下 (内節) あるいは上昇 (外節) している。ともに、視細胞の活動を抑制した状態 (右) では信号強度の変化が小さくなっている。

NFL: 神経線維層, GCL: 神経節細胞層, IPL: 内網状層, INL: 内顆粒層, OPL: 外網状層, ONL: 外顆粒層, PR-IS: 視細胞内節, PR-OS: 視細胞外節。

(文献¹¹⁾より改変して転載)

図3 ラット網膜の OCT イメージ
測定部位を b の矢印で示す。

NFL: 神経線維層, IPL: 内網状層, INL: 内顆粒層, OPL: 外網状層, ONL: 外顆粒層, PR-IS: 視細胞内節, PR-OS: 視細胞外節, RPE: 網膜色素上皮, CR: 脈絡膜。
(文献¹²⁾より改変して転載)

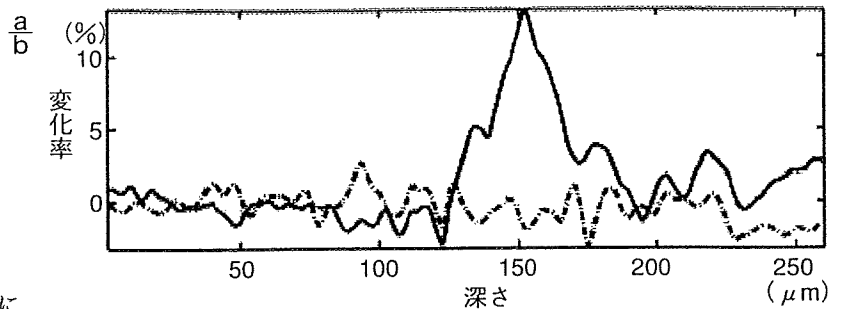
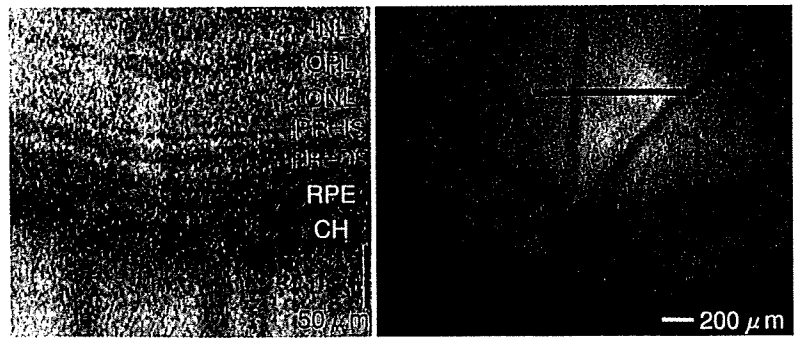
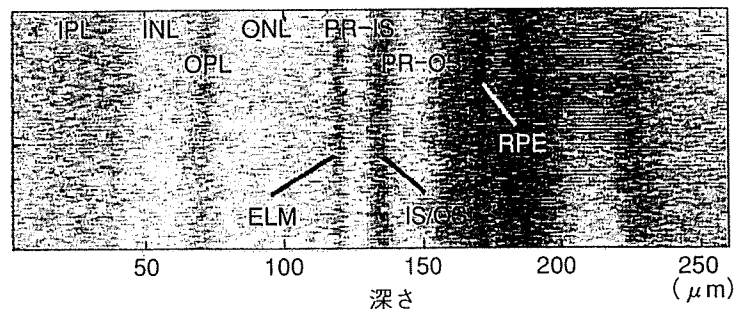


図4 暗順応状態での反射率の変化

a: 暗順応状態での反射率変化を深さ方向に表したものの。赤線は刺激後の反射率変化で、視細胞外節の反射率が選択的に10%以上上昇している。黒破線は刺激のない状態の反射率変化で、反射率の著明な変化はみられていない。

b: 対応する網膜断面図。

NFL: 神経線維層, IPL: 内網状層, INL: 内顆粒層, OPL: 外網状層, ONL: 外顆粒層, PR-IS: 視細胞内節, PR-OS: 視細胞外節, RPE: 網膜色素上皮, CR: 脈絡膜。
(文献¹²⁾より改変して転載)



によるフーリエドメイン OCT を用いた生体網膜 (ラット) の実験¹²⁾である。

Drexler らは、灌流液に浸した摘出ウサギ網膜を白色フラッシュで刺激し、OCT 信号の経時的変化を刺激なしの OCT 信号と比較している (中心波長 1,250 nm, バンド幅 150 nm, 深さ方向の解像度 3.5 μm, 白色フラッシュ刺激 200 ms, 図 1)。

視細胞層と内網状層の信号について解析を行い、特に視細胞外節の反射率が刺激後に増大していることに着目している (内節の反射率は反対に減少している)。また、この外層の反応はカリウム投与による視細胞機能のブロック後に消失することを示している (図 2)。

一方、Fujimoto らは、ネンブタール麻酔下の

ラット網膜を白色光で刺激し、OCT 信号を刺激なしのものと比較している (中心波長 890 nm, バンド幅 145 nm, 深さ方向の解像度 2.8 μm, 白色刺激 1.3s, 図 3)。刺激後の視細胞外節の反射率が 10% 以上上昇していることを示しているが、それ以外の層では OCT 信号の有意な変化はみられていない (図 4)。

Functional OCT の問題点

まず、functional OCT の信号は動きによるアーチファクトの影響を強く受けることが挙げられる。刺激前後の画像を重ね合わせて差分としての functional signal を抽出するため、記録中の画像の

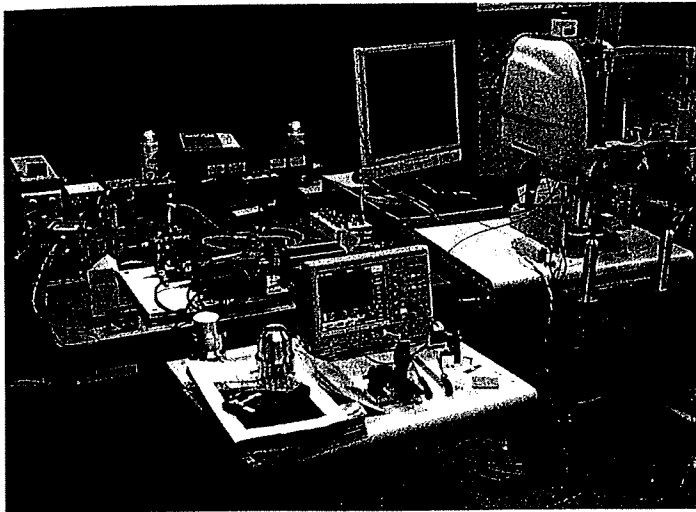


図5 東京医療センター，理化学研究所，(株)ニデックで共同開発中の functional OCT 試作器

Functional OCT と網膜内因性信号をともに記録することができる。

ズレが致命的になるのである。これは高解像度で functional imaging を行う場合に共通の問題点であるが、OCT は微細な構造を捉えているために特にその影響を受けやすい。解決策として、各画像間でピクセル値の相関を計算して位置合わせ (re-arrangement) を行うことや、OCT のスキャンスピードを速くすることなどが挙げられる。

次に、信号の発生起源が不明瞭な点である。動物種の違いがあるとはいえ、上述の2施設の実験結果を比べてみても、その信号の性質にはあまりの開きがある。特に、最近はさまざまな研究施設が覚醒下ヒトを用いた functional OCT の研究にも着手しているが、現時点での信号の質は、信号起源を論じるほどのレベルにはまったく達していない。Functional OCT は信号が小さいうえに、網膜内では光異性化に伴う早い反応から、血流増加に伴う遅い反応まで、起源を異にする信号が隣接する各層から惹起され、非常に複雑な光散乱変化が起きていることが予想される。Functional OCT を臨床的に意味のある検査法とするためには、まず麻酔下のより統制のとれた実験系を用いて、functional OCT でどのような生理学的現象が捉えられているのかを徹底的に調べ上げる必要がある。

Functional OCT の実用化は可能か

可能であろう。ただし、臨床現場での応用を数

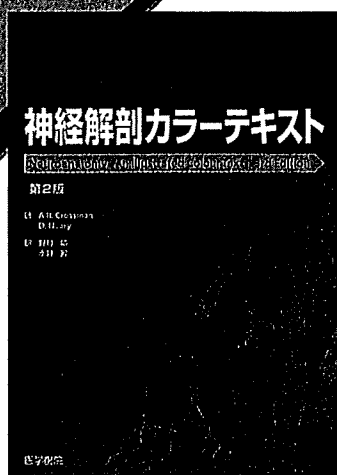
年以内に実現するのは難しいと思う。例えば LA-SIK で用いられるようなきわめて高周波数で位置ズレを補正するシステムや、補償光学 (adaptive optics) を利用して解像度を上げるシステムも、フラッシュ刺激後にヒトの眼底後極部で起こる微細で複雑な動きに対しては、現状では対処しきれない。また、現在のフーリエドメイン OCT よりもさらに高速のスキャンが可能な次世代 OCT の実用化が待たれているが、それだけでは上述の問題点を解決することはできない。しかし、これらの問題点を1つ1つクリアしていけば、必ず近い将来にゴールは見えてくるものと筆者らは考えている (図5)。

文献

- 1) Maheswari RU, Takaoka H, Homma R et al : Implementation of optical coherence tomography (OCT) in visualization of functional structures of cat visual cortex. *Opt Comm* 202 : 47-54, 2002
- 2) Maheswari RU, Takaoka H, Kadono H et al : Novel functional imaging technique from brain surface with optical coherence tomography enabling visualization of depth resolved functional structure in vivo. *J Neurosci Methods* 124 : 83-92, 2003
- 3) Cohen L : Changes in neuron structure during action potential propagation and synaptic transmission. *Physiol Rev* 53 : 373-418, 1973
- 4) Harary H, Brown E, Pinto H : Rapid light-induced changes in near infrared transmission of rods in *Bufo marinus*. *Science* 202 : 1083-1085, 1978
- 5) Grinvald A, Lieke E, Frostig RD et al : Functional architecture of cortex revealed by optical imaging of intrinsic signals. *Nature* 324 : 361-364, 1986

- 6) Tsunoda K, Yamane Y, Nishizaki M et al : Complex objects are represented in macaque inferotemporal cortex by the combination of feature columns. *Nat Neurosci* 4 : 832-838, 2001
- 7) Tsunoda K, Oguchi Y, Hanazono G et al : Mapping cone- and rod-induced retinal responsiveness in macaque retina by optical imaging. *Invest Ophthalmol Vis Sci* 45 : 3820-3826, 2004
- 8) Hanazono G, Tsunoda K, Shinoda K et al : Intrinsic signal imaging in macaque's retina reveals different types of flash-induced light reflectance changes of different origins. *Invest Ophthalmol Vis Sci* 48 : 2903-2912, 2007
- 9) Inomata K, Tsunoda K, Hanazono G et al : Distribution of retinal responses evoked by trans-scleral electrical stimulation detected by intrinsic signal imaging in macaque monkeys. *Invest Ophthalmol Vis Sci* 49 : 2193-2200, 2008
- 10) Hanazono G, Tsunoda K, Kazato Y et al : Evaluating neural activity of retinal ganglion cells by flash-evoked intrinsic signal imaging in macaque retina. *Invest Ophthalmol Vis Sci* (in press)
- 11) Bizheva K, Pflug R, Hermann B et al : Optophysiology : depth-resolved probing of retinal physiology with functional ultrahigh-resolution optical coherence tomography. *Proc Natl Acad Sci USA* 103 : 5066-5071, 2006
- 12) Srinivasan VJ, Wojtkowski M, Fujimoto JG et al : In vivo measurement of retinal physiology with high-speed ultrahigh-resolution optical coherence tomography. *Opt Lett* 31 : 2308-2310, 2006

豊富なカラー写真と図版を掲載した神経解剖学の入門書



神経解剖カラーテキスト 第2版

著 A. R. Crossman / D. Neary
訳 野村 巖・水野 昇

豊富なカラー写真と図版を掲載した神経解剖学のテキスト。基礎知識を簡潔に解説し、神経疾患の病因と臨床診断法のアウトラインを知るための初歩的な臨床的概念を多数紹介。今版では巻末に症例を基にした問題集が設けられ、知識の定着を確認できる。神経解剖学の全体を概観したいと願う医学生やPT、OT、STを目指す学生にとっての優れた入門書。脳実習の参考書としても有効。

●A4 頁224 2008年 定価5,880円(本体5,600円+税5%) [ISBN978-4-260-00579-1]
消費税率変更の場合、上記定価は税率の差額分変更になります。



医学書院

〒113-8719 東京都文京区本郷1-28-23 [販売部] TEL: 03-3817-5657 FAX: 03-3815-7804
E-mail: sd@igaku-shoin.co.jp http://www.igaku-shoin.co.jp 振替: 00170-9-96693

REVIEW

Origins of Retinal Intrinsic Signals: A Series of Experiments on Retinas of Macaque Monkeys

Kazushige Tsunoda^{1,2}, Gen Hanazono^{1,2}, Koichi Inomata^{1,2}, Yoko Kazato^{1,2},
Wataru Suzuki², and Manabu Tanifuji²

¹Laboratory of Visual Physiology, National Institute of Sensory Organs, Tokyo, Japan;
²Laboratory for Integrative Neural Systems, Riken Brain Science Institute, Saitama, Japan

Abstract

Diffuse flash stimuli applied to the ocular fundus evoke light reflectance decreases of the fundus illuminated with infrared observation light. This phenomenon, which is independent of the photopigment bleaching observed as an increase in the reflectance of visible light, is called intrinsic signals. Intrinsic signals, in general, are stimulus-evoked light reflectance changes of neural tissues due to metabolic changes, and they have been extensively investigated in the cerebral cortex. This noninvasive objective technique of functional imaging has good potential as a tool for the early detection of retinal dysfunction. Once the signal properties were studied in detail, however, it became apparent that the intrinsic signals observed in the retina have uniquely interesting properties of their own due to the characteristic layered structure of the retina. Experiments on anesthetized macaque monkeys are reviewed, and the possible origins of the intrinsic signals of the retina are discussed. *Jpn J Ophthalmol* 2009;53:297-314
© Japanese Ophthalmological Society 2009

Key Words: functional imaging, intrinsic signals, monkey, optical imaging, retina

Introduction

Recent advances in imaging techniques, such as scanning laser ophthalmoscopy (SLO) and optical coherent tomography (OCT),¹⁻⁴ have revealed the morphology of retinal structures with very fine spatial resolution. However, objective functional assessment of the retina is also essential to the understanding of the physiology of the retina and for correct diagnoses and prognoses of various retinal disorders.

Almost 50 years ago, the densities of cone and rod photopigments were assessed quantitatively by measuring the changes of visible light reflected from the retina by observing either the bleaching process following dark adaptation or the regeneration process following a full bleach.⁵⁻¹⁰ Retinal densitometry has been used to map the function of both the normal and the diseased retina, by using either a

fundus camera¹¹⁻¹⁵ or SLO.¹⁶⁻¹⁸ However, the clinical applications of these techniques are limited because of technical limitations.

Intrinsic signal imaging with an infrared observation light, on the other hand, is of considerable value in constructing a wide-field topographic map of the neural functions of the retina because the light reflectance can be monitored by nonvisible light. This technique is not invasive, and is free from inhomogeneous reflections from both the internal limiting membranes and the nerve fiber layers, which lead to considerable artifacts when measurements are conducted with visible light.

Optical imaging based on intrinsic signals is a well-established technique for assessing neuronal activity, and has been widely used during the last two decades to map the functional organization of various areas of the visual cortex,¹⁹ including the primary visual cortex (V1),^{20,21} V2,²² V4,²³ M1,²⁴ and TE.²⁵ In these studies, neural activation led to a decrease in light reflectance recorded from the cortical surface by a charge-couple device (CCD) camera without the need for any extrinsic probes. The reflectance changes are due to multiple metabolic changes following neural activity, such as blood volume changes in the capillaries

Received: January 19, 2009 / Accepted: March 16, 2009

Correspondence and reprint requests to: Kazushige Tsunoda, Laboratory of Visual Physiology, National Institute of Sensory Organs, 2-5-1 Higashigaoka, Meguro-ku, Tokyo 152-8902, Japan
e-mail: tsunodakazushige@kankakuki.go.jp

(observation light, 540 nm), changes in the oxygenated levels of hemoglobin (600–650 nm), and changes in tissue light scattering (infrared light).^{26,27} Although the reflectance changes are not a direct measure of the neural activity, the intrinsic signals correspond well with the neural activity examined by conventional extracellular recording.^{25,28,29}

This technique has been recently used to investigate the cone- and rod-generated responses of the retina of macaque monkeys (Fig. 1),³⁰ humans,^{31–33} and cats³⁴ with an infrared observation light. The source of retinal intrinsic signals might be attributed to metabolic changes such as in the cerebral cortex²⁷ or to the stimulus-induced scattering changes in the near infrared as in the isolated retina.^{35,36} It is apparent, however, that the intrinsic retinal signals observed in the in situ retina have their own characteristic properties due to the complex layered structure and topographic differences of the retina. Thus, before the retinal intrinsic imaging technique can be brought into the clinic, a detailed knowledge of the properties and origin of the signals is needed. Here, the results of experiments on the retina of anesthetized macaque monkeys are reviewed, and the possible sources of the intrinsic signals discussed. We shall summarize the results of each of five experiments designed to investigate the properties and origin of the intrinsic signals of the monkey's retina:

1. The intrinsic signals and the electroretinograms (ERGs) evoked by the same flash stimuli were recorded under different stimulus conditions.³⁷
2. The intrinsic signals were elicited by transscleral electrical stimulation of the retina by DTL electrodes. The effects of changing the intensity and frequency of the electrical currents were investigated.³⁸
3. The intrinsic signals from the optic disc and primary visual cortex (V1) were measured simultaneously with different wavelengths of observation lights to determine the contribution of the level of blood oxygenation on the intrinsic signals.³⁹
4. The retinal blood flow was measured by laser Doppler flowmetry, and the time courses of the intrinsic signals and blood flow changes elicited by the same stimuli, were compared.³⁹
5. The flash-induced retinal intrinsic signals were measured before and after an intravitreal injection of tetrodotoxin (TTX) to determine the contribution of neuronal spike activities in the inner retina to the intrinsic signals.³⁹

General Methods

The procedures used to record the intrinsic signals have been described in detail.^{30,37–39} The experiments were performed on rhesus monkeys (*Macaca mulatta*) and Japanese monkeys (*Macaca fuscata*). Following an intramuscular injection of atropine sulfate (0.08 mg/kg), the monkeys were anesthetized with droperidol (0.25 mg/kg) and ketamine (5.0 mg/kg), and then paralyzed with vecuronium bromide (0.1–0.2 mg/kg per hour). They were artificially

ventilated with a mixture of 70% N₂O, 30% O₂, and 1.0%–1.5% isoflurane. The electroencephalograph (EEGs), electrocardiograms (ECGs), expired CO₂, and rectal temperature were monitored throughout the experiments. Before the recordings, the pupils were fully dilated with topical tropicamide (0.5%) and phenylephrine hydrochloride (0.5%). The experimental protocol was approved by the Experimental Animal Committee of the Riken Institute, and all experimental procedures were carried out in accordance with the guidelines of the Riken Institute and the ARVO Statement for the Use of Animals in Ophthalmic and Vision Research.

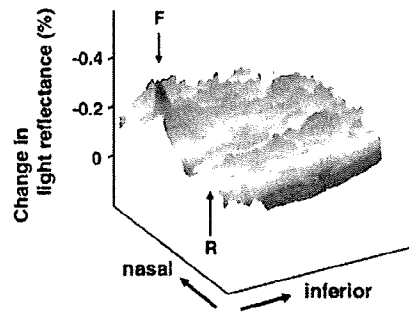
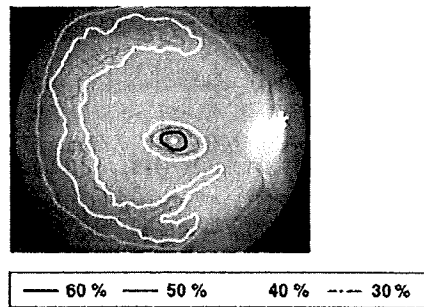
A modified digital fundus camera system (NM-1000, Nidek, Aichi, Japan) was used to observe and measure the light reflectance changes from the ocular fundus. The fundus images were recorded with a CCD camera (PX-30BC, Primetech Engineering, Tokyo, Japan), and the images were digitized with an IBM/PC-compatible computer equipped with a video frame grabber board (Corona II, Matrox, Dorval, Quebec, Canada; gray level resolution, 10 bits; spatial resolution, 640 × 480; temporal resolution, 1/30 s). The camera was focused on the macular vessels, and the area recorded covered 45° and included the macula, superior and inferior vascular arcades, and the optic disc.

The ocular fundus (the cerebral cortex in experiment 3) was continuously monitored with light from a halogen lamp filtered through either an infrared (870 ± 30 nm) or a visible (570 ± 10 nm, or 630 ± 20 nm in experiment 3) interference filter (Fig. 2). Each recording trial consisted of 300 (450 in experiment 5) video frames collected at 30 frames/s for a total recording time of 10 s (15 s in experiment 5). An unfiltered xenon flash (duration, 1 ms) stimulated the entire posterior pole 500 ms after the initiation of data acquisition. The maximal flash intensity (0 log unit intensity) measured at the cornea was 3.08 × 10² cd-s/m² (measured at 50.2 mm from the object lens by a photoradiometer: IL-1700, International Light Technologies, Peabody, MA, USA). The timing of the data acquisition and stimulus delivery was controlled by a computer.

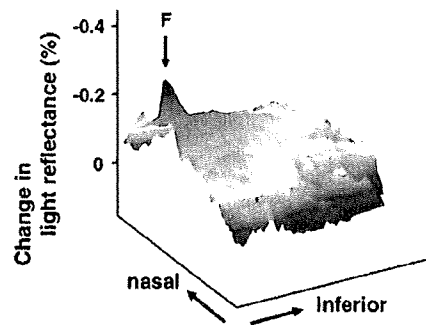
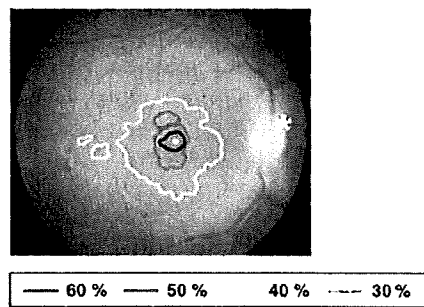
The changes in light reflectance from the ocular fundus following the stimulus consisted of either a darkening (decrease in light reflectance) or a brightening (increase in light reflectance) of the retina. Under infrared observation, the light reflectance of the entire posterior retina decreased following a flash stimulus; that is, fundus images became darker (Fig. 3B). The optical signals were calculated as follows: (1) the gray-scale values of the images obtained after the stimulus were divided by those obtained during a 0.5-s period before the stimulus pixel by pixel, and (2) each value (ratio) was rescaled to a 256-level gray-scale resolution to show the stimulus-induced reflectance changes.

Three retinal sites were investigated: (1) the fovea; (2) the posterior retina between the macula and inferior temporal artery; and (3) the optic disc (Fig. 3A). In experiment 2, a region twice as large as that designated by F in Fig. 3A was used to analyze the time course because the signal-to-noise ratio was too low to analyze the time course of the smaller foveal region. The time course of the intrinsic signals

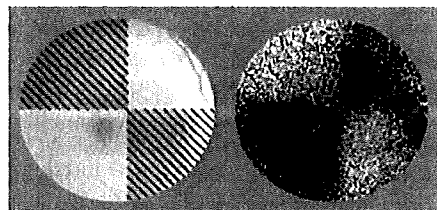
A Dark-adapted



B Light-adapted



C



D

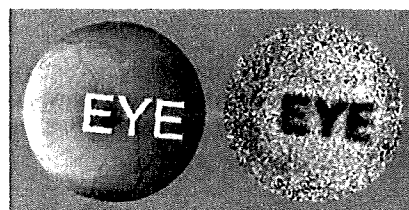


Figure 1A–D. Retinal intrinsic signals recorded from the retina of a Macaque monkey. **A Left:** response topography of the intrinsic signal evoked by a diffuse flash under dark-adapted condition. The foveal center is indicated by a white dot, and * indicates the optic disc. Regions with 60%, 50%, 40%, and 30% of the peak signal intensity value at the fovea are outlined by different colors. **Right:** pseudocolor topographic map of light reflectance changes in the inferior retina under dark-adapted condition profiled along the horizontal meridian. *F*, the location of the fovea; *R*, the peak of the rod ring. To emphasize the negative peak, we used graphical scaling opposite to conventional methods. Modified from Tsunoda et al., *Invest Ophthalmol Vis Sci*,³⁰ with permission. **B Left:** topographic map of the intrinsic signal evoked by a diffuse flash under light-adapted condition. **Right:** pseudocolor topographic map of light reflectance changes in the inferior retina under light-adapted condition. Modified from Tsunoda et al., *Invest Ophthalmol Vis Sci*,³⁰ with permission. **C** Intrinsic signals evoked by a focal stimulus. **Left:** mosaic-like focal stimulus in the posterior pole is shown on a fundus image. The stimulus was blocked over the hatched area. **Right:** two-dimensional image of the intrinsic signals evoked by a focal stimulus, averaged from 6.5 to 9.5 s following stimulation (single trial). **D** Intrinsic signals evoked by a focal flash stimulus. **Left:** the word "EYE" was projected onto the posterior pole by a brief flash. **Right:** two-dimensional image of the intrinsic signal (single trial). The focally stimulated region shows a decrease in the light reflectance following the stimulus, and this darkened region matched the location of the focal stimulus exactly. Note that the light reflectance in the nonstimulated area of the posterior pole was much higher (brighter) than the prestimulus level, which is not observed when a diffuse stimulus is used.

evoked by a brief flash stimulus was different for each region of the ocular fundus. A representative flash-evoked response from a single stimulus under the dark-adapted condition is shown in Fig. 3C. The reflectance changes at the fovea were rapid and reached a negative peak (darkening) within 100–200 ms following the flash. The darkening then gradually returned to the prestimulus baseline level.

The changes in the signals at the optic disc were much slower and reached a peak 5–6 s following the flash. The signals in the nonfoveal posterior retina had both fast and slow components. The light reflectance decreased rapidly within 100 ms to a flexural point, and then decreased more slowly to reach a trough 5–6 s following the flash. The time course of the intrinsic signals of the posterior retina was

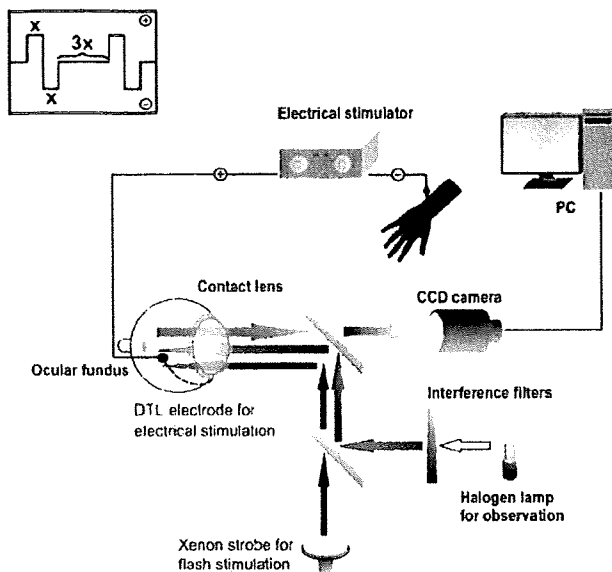


Figure 2. Schematic drawing of the experimental set-up and pattern of electrical pulses. The ocular fundus is illuminated by light from a halogen lamp filtered through a band-pass interference filter and monitored by a CCD camera. Stimulus was given either by a xenon flash through the objective lens of the fundus camera or by an electric current through a DTL electrode placed on the conjunctiva. *Inset.* Biphasic pulse current with a duration of x is followed by a resting period as long as $3x$. As the frequency is changed from 5 to 100 Hz, x is changed from 40 to 2 ms. Modified from Tsunoda et al., *Invest Ophthalmol Vis Sci.*, with permission.

approximately the same over the whole field except for the small central region within the 300- μ m avascular foveal area (Fig. 3D). The light reflectance at the fovea did not continue decreasing after the initial negative peak.

Experiment 1

This experiment was designed to investigate the properties of the four components of flash-evoked intrinsic signals. The intrinsic retinal signals and the electroretinograms (ERGs) are compared.

The time course and amplitudes of the retinal intrinsic signals and the ERGs evoked by the same diffuse flash stimulus were compared under different flash intensities and flash intervals. The maximum luminance of the xenon flash was 3.08×10^2 cd-s/m², and neutral density filters were used to attenuate the luminance. The intrinsic signals and ERGs were recorded over an 8.8 log unit range in 11 steps, namely, -8.8, -7.8, -6.7, -6.0, -4.8, -3.7, -3.0, -1.8, -0.7, -0.3, and 0.0. The recordings were performed consecutively with 20-min intervals between changes in the intensity under both dark- and light-adapted conditions. In the light-adapted condition, each recording was followed by 10 min of light adaptation with diffuse illumination of the retina of 30 cd/m².

To examine the effects of interstimulus intervals, the retina was dark-adapted for 30 min and then bleached by a

strong white flash of 1.54×10^2 cd-s/m². The intrinsic signals and ERGs were elicited with a flash of the same intensity as the bleaching flash following intervals of 0.5, 1.0, 3.0, 5.0, 10, 30, and 60 min.

To quantify the flash-induced intrinsic signals, the value of the initial peak of light reflectance change at the fovea (F; 15×15 pixels), either the value at the flexural point of light reflectance change (R1) or the value at the end of the recording trial (R2) in the inferior retina (60×40 pixels), and the lowest value of light reflectance at the optic disc (D; $\sim 70 \times 50$ pixels) (Fig. 3C) were used.

A bipolar contact lens electrode (Mayo, Aichi, Japan) was used to record the ERGs. The ERGs were amplified $\times 10000$, and low and high band-pass filters were set at 0.3 and 500 Hz (Power Lab, ADInstruments, Colorado Springs, CO, USA). A 45° white xenon flash stimulus was delivered through the same optical system to stimulate the retina while the fundus was monitored with the infrared observation light. As in intrinsic signal imaging, two ERGs were recorded for each recording condition, and the responses were averaged for analyses.

Effects of Stimulus Intensity

The intrinsic signals and the ERGs recorded following the diffuse flash are shown in Figs. 4A, 5A, and 6A. The changes in the intensities of the intrinsic signals and the ERG amplitudes are shown in Figs. 4B, 5B, and 6B. Under dark-adapted conditions (Fig. 4), the amplitudes of the a and b waves of the ERGs increased as the stimulus intensity increased. The intrinsic signals of D and R2 had the same threshold as the b wave, and their amplitudes also increased with the intensity. The amplitudes of D and R2 reached a plateau at -6.0 log units, and D did not change significantly with higher intensities. R2 increased again with flash intensities over -1.8 log units. The threshold of R1 was higher than that of D, R2, or the a wave of the ERG, and the amplitude of R1 increased gradually with the increase in flash intensity. The amplitude of F also increased with the flash intensity and its threshold was higher than that of any other intrinsic signal.

Under light-adapted conditions, the amplitudes of the a and b waves increased progressively with an increase in flash intensity, but that of the b wave decreased with intensities higher than -3.0 log units because of the photopic hill phenomenon seen in ERG recordings (Fig. 5B).¹⁰ The thresholds of D and R2 of the intrinsic signal images were 2.1 log units higher than those under dark-adapted conditions. The thresholds of D were the same as those of R2 and the a and b waves. The thresholds of R1 and F did not differ under both dark- and light-adapted conditions.

The intrinsic signals evoked by a dim flash (weaker than -6.0 log units) under dark-adapted conditions reflected the activation of rod photoreceptors, and those evoked by a stronger flash reflected the activities of both cone and rod photoreceptors. The intrinsic signals evoked under light-

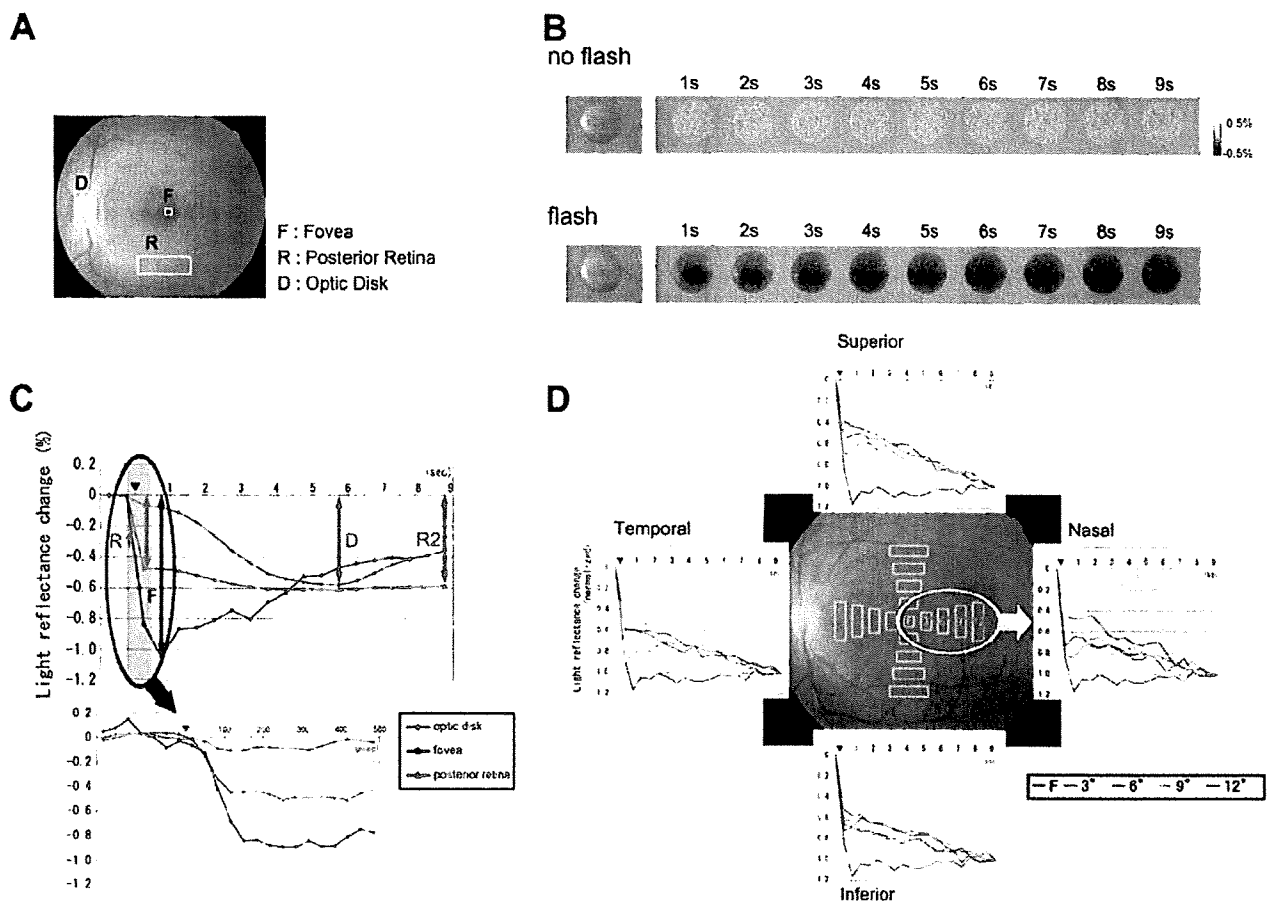


Figure 3A–D. Fundus photograph and time courses of intrinsic signals following a flash stimulus. **A** Fundus photograph of normal retina showing the regions analyzed. **B** Time courses of two-dimensional images of the ocular fundus showing the light reflectance changes during a 10 s trial with (lower) and without (upper) flash stimulus. Images on the left are fundus images taken at the beginning of the trial. Images on the right show the light reflectance changes following a flash. Darkened regions indicate a decrease in light reflectance following flash stimulus. Thirty consecutive video frames collected during 1 s were averaged for one poststimulus fundus image. **C** Plot of the time courses of light reflectance changes in a single trial following a diffuse flash stimulus in the three locations shown in **A**. The time following the flash is shown on the abscissa. The delivery of the flash is indicated by the arrowhead. Each point is the average of 15 video frames collected during 0.5 s of light reflectance changes. **F**, signal at fovea; **D**, signal at optic disc; **R1** and **R2**, signals in the nonfoveal posterior retina (colored arrows). The time course of the reflectance changes during the first 500 ms following a flash is shown in the lower graph, where each point is the average of two video frames during 1/15 s. **D** Time courses of light reflectance changes in a single trial following a diffuse flash measured at the fovea and four different regions within 12° from the fovea in each quadrant. Amplitudes are indicated as values relative to the light reflectance changes at the end of each trial (1.0). The four regions tested in each quadrant are indicated as distances from fovea (3°, 6°, 9°, and 12°). Modified from Tsunoda et al., *Invest Ophthalmol Vis Sci*,³⁷ with permission.

adapted conditions reflected the activation of cone photoreceptors (Fig. 1A and B).

Effects of Flash Intervals

Following bleaching by a bright flash, the amplitudes of the a and b waves were reduced. These amplitudes then increased in the dark with an increase in time (Fig. 6).^{11,12} Flash intensity was 1.7 log units more than that of the International Society of Clinical Electrophysiology of Vision (ISCEV) standard bright flash, which resulted in a slower recovery of the ERG amplitudes. For the intrinsic signals,

only the F signal had a pattern similar to that of the ERGs; that is, the amplitude increased gradually with longer intervals in the dark following the preceding flash. On the other hand, D, R1, and R2 peaked at 3–5 min following the preceding flash. These findings indicate that the source of the intrinsic signals of the optic disc and the nonfoveal posterior retina is different from that of the fovea.

The properties of the R2 signal were similar to those of the D signal (Figs. 4B and 5B). Thus, the inner retina may be the main contributor to the D and R2 signals because these slow signals could not be observed at the fovea, which lacks both inner retinal layers and blood vessels.⁴³ The slow time course of the D and R2 signals are probably related to

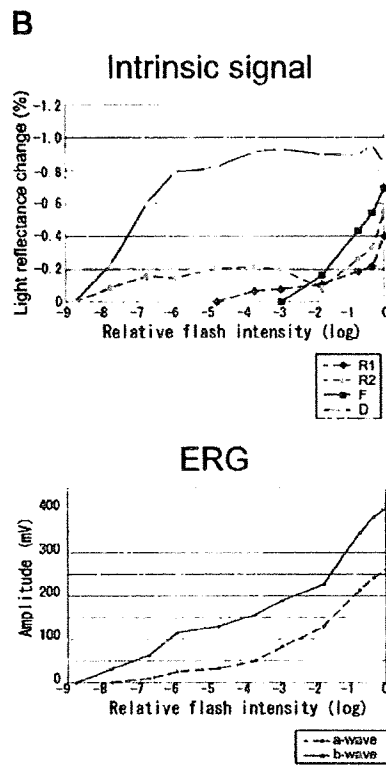
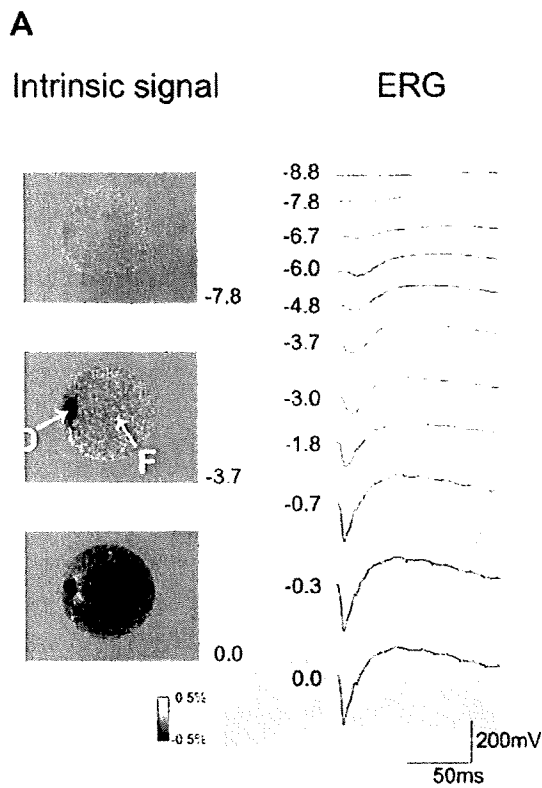


Figure 4A, B. Intrinsic signal images and electroretinograms (ERGs) evoked by a diffuse stimulus under dark-adapted conditions. **A** Fundus images of the intrinsic signals (*left*) and ERGs (*right*) following a diffuse flash in the dark-adapted condition with stimulus intensities from -8.8 to 0 log unit. Intrinsic signal images from a single trial averaged from 5.0 to 8.0 s following the flash are shown on the left. The darkened region in fundus images indicates a light reflectance decrease following the flash. The relative log flash intensities to the maximum flash are indicated. *D*, optic disc; *F*, fovea. **B** Amplitudes of R1, R2, F, and D of the intrinsic signals to increasing flash intensities are shown as light reflectance changes in the upper graph. The amplitudes of the ERG a and b waves with the same stimulus series are shown in the lower graph. Note that negative values of light reflectance changes are plotted to indicate the strength of intrinsic signals (also in Figs. 5, 6, and 7). Modified from Tsunoda et al., Invest Ophthalmol Vis Sci,³⁷ with permission.

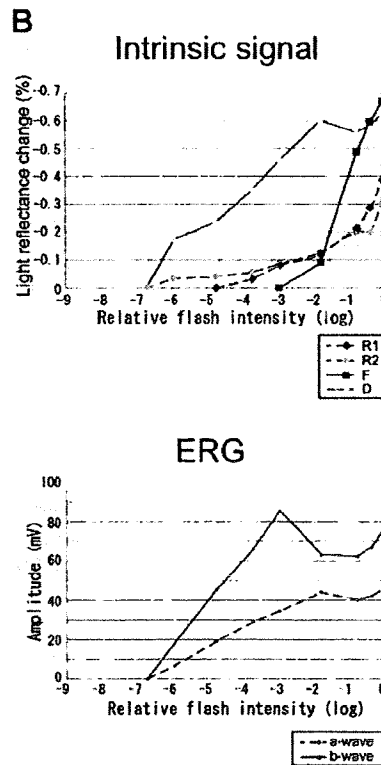
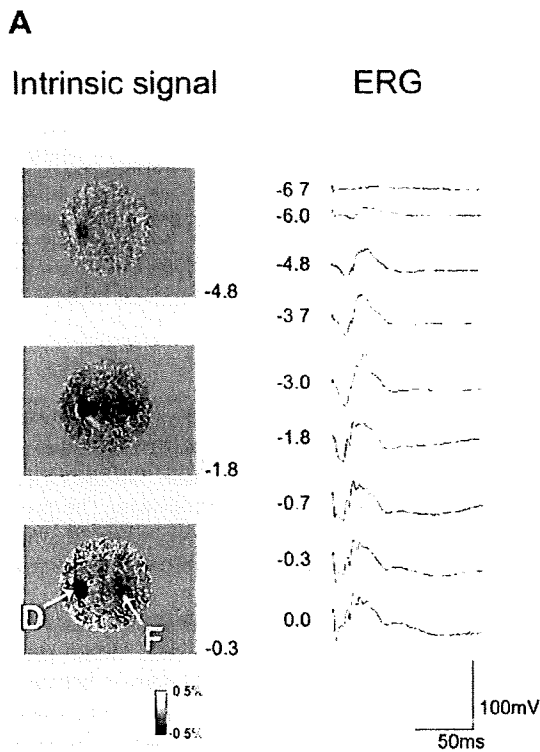


Figure 5A, B. Intrinsic signals and ERGs following a diffuse stimulus under light-adapted conditions. **A** Fundus images of the intrinsic signals (*left*) and ERGs (*right*) following different stimulus intensities (-6.7 to 0 log unit intensity). Representative signal images for a single trial averaged 5.0 to 8.0 s following a flash are shown. **B** Amplitudes of R1, R2, F, and D of the intrinsic signals and the a and b waves of the ERGs to various flash intensities as shown in Fig. 4. Modified from Tsunoda et al., Invest Ophthalmol Vis Sci,³⁷ with permission.

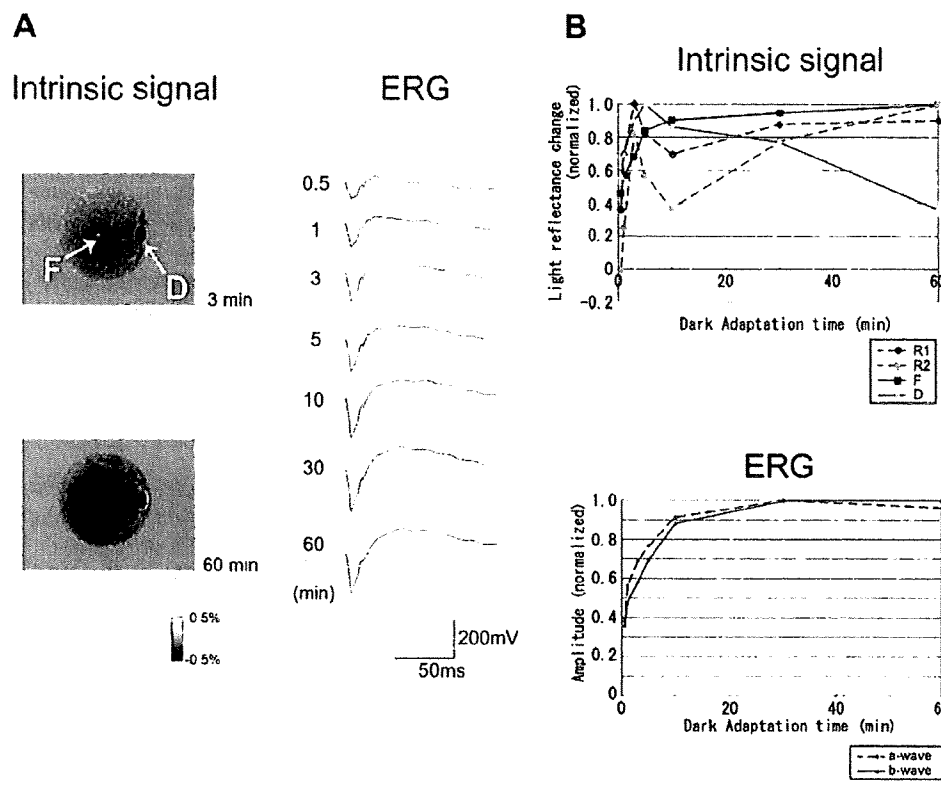


Figure 6A, B. Intrinsic signals and ERGs following a diffuse stimulus recorded at different times following bleaching. **A** Fundus images of intrinsic signals (left) and ERGs (right) evoked by a diffuse flash (-0.3 log units) at different intervals (0.5 to 60 min) following a bleaching flash of the same intensity. Representative images from a single trial averaged from 5.0 to 8.0 s following a flash are shown. **B** Amplitudes of R1, R2, F, and D of the intrinsic signals and a and b waves of the ERGs at different flash intervals. Amplitudes are indicated as relative values of the maximum for each signal component. Modified from Tsunoda et al., *Invest Ophthalmol Vis Sci*,³⁷ with permission.

a flash-induced blood flow increase because the reflectance changes were three times greater in the central region of the optic disc occupied by the central retinal artery and vein than in other regions of the optic disc, although the time course was almost the same in all locations within the optic disc.³⁷ Interestingly, the amplitudes of the D and R2 signals were largest with flash intervals of 3–5 min (Fig. 6B), very different from the results of the ERGs. It is possible that the mechanism by which neural activity is converted to a vascular response, that is, neurovascular coupling,^{44,45} is activated most effectively when the stimuli are given repeatedly at intermediate intervals.

The unique morphological structure of the fovea, namely, the absence of rod photoreceptors, capillaries, and other inner retinal layers, indicates that the F signal reflects the activation of cone photoreceptors under all recording conditions. Because the foveal avascular region is free of capillaries and therefore not subject to changes in either hemoglobin concentration or blood flow following neural activation, the source of the F signals is probably the light scattering changes due to the microstructural changes following activation of the cone photoreceptors.¹³ These light scattering changes are thought to arise from the structural changes in the outer segment discs, membrane hyperpolarization, cell swelling, and changes in the composition of the interphotoreceptor matrix.^{36,38} Another hypothesis, that changes in choroidal blood flow are the source of the foveal signals, was proven wrong by the results of experiment 4.

The threshold of R1 lies between the thresholds of the optic disc and fovea, and remained unchanged under both dark- and light-adapted conditions. This result suggests that the cone photoreceptors were the main contributors to the R1 signal, because bleaching of the rods in the light-adapted condition did not change the threshold of R1. It is, however, difficult to assume that rod and cone photoreceptors play different roles in light reflectance changes.

The property of the R1 signal is complicated in another way. The abrupt darkening of the intrinsic image following each flash may be suitably explained by photoreceptor responses similar to the F signal, but the results shown in Fig. 6B suggest that R1 shares the same signal origin with the D and R2 signals. Thus, although the data do not provide any evidence for the exact source, it is suggested that the R1 signal originates not only in the photoreceptors but also in either the inner or the middle retinal layer elements.

Experiment 2

This experiment was designed to determine whether the slow intrinsic signals can be evoked without photic stimulation of photoreceptors. Intrinsic signals were elicited by transscleral electrical stimulation of the retina.

If the slow light reflectance changes at the optic disc and retina in experiment 1 reflect inner retinal activities, similar responses should be observed by direct electrical

stimulation of the inner retina without photoreceptor activation. In this experiment, intrinsic signals were evoked by transscleral electrical stimulation with DTL fiber electrodes.⁷ The effects of changing the intensity and frequency of the stimulating electrical current were investigated.

Electrical pulses were delivered by DTL electrodes because electrical phosphenes are believed to be more homogeneous and continuous with a DTL electrode than with a contact lens electrode.¹⁸ The fibers of the DTL electrode were placed on the lower bulbar conjunctiva 5.0 mm from the corneal limbus. The conjunctiva was covered with 3% hyaluronic acid and 4% chondroitin sulfate (Viscoat, Alcon Japan, Tokyo, Japan), and the reference electrode was placed on the ipsilateral wrist (Fig. 2). Biphasic electrical pulses were used for all experiments (inset, Fig. 2). The stimulus consisted of a positive current for x ms followed by a negative current for x ms, and then a rest period for $3x$ ms. In most experiments the pulse frequency was set at 20 Hz and x was set to 10, but whenever the pulse frequency was changed, x varied from 40 (at 5 Hz) to 2 (at 100 Hz) in order to keep the total current constant. The stimuli were delivered for 0.5 s following the initiation of data acquisition for 1.0 s. The pulse duration and frequency were controlled by a function generator (Multifunction Synthesizer WF 19443B, NF Corporation, Yokohama, Japan). In order to compare the responses evoked by light flashes, white flickering flashes (20 Hz) were administered to the entire posterior pole of the ocular fundus for 1.0 s beginning 0.5 s after the initiation of data acquisition. The flash intensity measured at the cornea was 6.07 cd/s/m².

Electrical stimulation evoked a uniform change in reflectivity across the posterior pole of the retina, and the spatial distribution did not reflect the anatomical distribution of cone and rod photoreceptors as it did with light stimulation.³⁸ The intrinsic signal did not peak at the fovea, and the perimacular response under dark-adapted conditions did not differ significantly from that under light-adapted conditions. The time course of the signals from the three regions evoked by electrical pulses (20 Hz, 1.0 s, 500 μ A) under dark-adapted conditions is shown in Fig. 7A. The light reflectance changes in the macula and perimacular retina were as slow as that at the optic disc. Although the onset of light reflectance changes in the perimacular retina slightly preceded that at the optic disc, the signals in the three regions reached their negative peaks 5–6 s following the stimulus.

The effect of currents ranging from 0 to 1000 μ A on the intrinsic signals was determined under both dark- and light-adapted conditions (pulse frequency, 20 Hz; stimulus duration, 1 s; pulse duration, 10 ms; Fig. 7B). The peak light reflectance value obtained during the 10-s recording was used as the signal amplitude for each current (as in Fig. 7C), and the results of the three trials were averaged. The response properties appeared to be approximately the same in each region under both dark- and light-adapted conditions. The change in the reflectance as a function of the

electrical current was sigmoidal; weak signals were recorded at low currents from 100 to 400 μ A, stronger signals appeared above 400 μ A, and maximum signals above 600 μ A. The threshold of the electrically evoked intrinsic signals was probably lower than 100 μ A in each of the three regions, but it was technically difficult to determine the peak value of each signal when the absolute light reflectance change was < 0.05%. A small difference in the signal amplitudes between dark- and light-adapted conditions in the perimacular area was visible (middle graphs in Fig. 7B), yet the difference was not significant with respect to amplitude or threshold when compared with the flash-evoked responses, where a two- to fivefold difference in the signal amplitude and a 2.1 log unit difference in the threshold of flash intensity were observed between dark- and light-adapted conditions (Figs. 4 and 5).

The intrinsic signals evoked by different electrical stimulus frequencies under dark-adapted conditions were then measured, (stimulus current, 500 μ A; stimulus duration, 1 s; pulse frequency (Hz)/pulse duration (ms), 5/40, 10/20, 15/13.3, 20/10, 40/5, 60/3.33, 80/2.5, and 100/2; Fig. 7C). The results of the five trials were averaged. The response properties seemed to be almost the same in each region: the intrinsic signals were maximal when the current frequency was 15 or 20 Hz. The signal was reduced when the frequency was either increased or decreased.

A number of studies, mainly experiments using isolated retinas, have investigated the retinal sites activated by electrical stimuli. Most of these studies have shown that the site activated was more proximal than the photoreceptors, for example, synaptic terminals of the photoreceptor cells,⁴⁹⁻⁵¹ bipolar cells,⁵²⁻⁵⁵ horizontal cells,^{56,57} amacrine cells,⁵⁸ and retinal ganglion cells.^{51,55,59} Experiments by Potts and colleagues using electrically evoked potential (EER) show that the site of transscleral electrical activation was more central than the photoreceptors,⁶⁰⁻⁶² and Miyake and colleagues have shown that the retinal origin of EER lies either in the middle layer of the retina or close to the retinal ganglion cell layer.⁶³⁻⁶⁶ Brindley carefully examined the strength and extent of the electrical phosphenes, and concluded that the electrical phosphenes did not result from stimulation of the optic nerve fibers.⁶⁷

With changes in the frequency of the electrical pulses, the maximal signals were obtained when the current frequency was 15–20 Hz regardless of the recording region in the ocular fundus. Toi and Riva⁶⁸ presented an achromatic checker board pattern to anesthetized cats. They found that the stimulus-related blood flow increases measured by laser Doppler flowmetry were maximal when the stimulus frequency was 20 Hz.⁶⁸ The blood flow increase at the optic nerve head following diffuse luminance flicker had similar physiological properties to those of magnocellular retinal ganglion cell neural activities.^{69,70} On the basis of these data, Riva et al.⁷¹ measured the blood flow increases following a 15-Hz flicker stimulus in patients with ocular hypertension and early glaucoma, and found that the flicker-evoked blood flow changes were abnormally reduced. Psychophysical studies using flickering stimuli,⁷² electrical phosphenes,⁷³

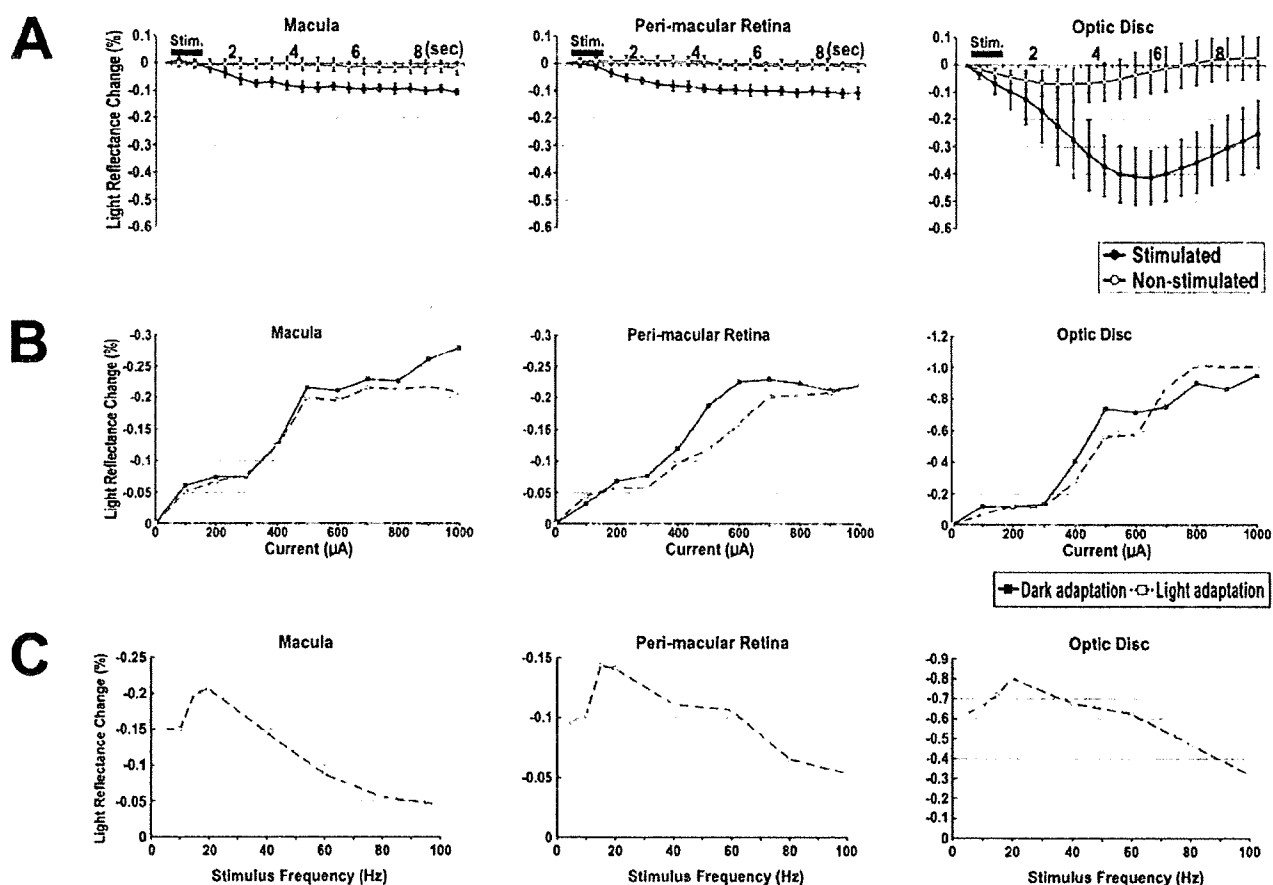


Figure 7A–C. Intrinsic signals evoked by transscleral electrical stimulation. **A** Plot of time courses of the light reflectance changes evoked by electrical stimulation at three different regions in a normal eye. The period of stimulus delivery (1.0 s) is indicated by the *thick bars*. The time following the initiation of stimulus is shown on the abscissa. Data of ten consecutive trials are averaged. **B** Stimulus intensity and intrinsic signals. Changes in the intrinsic signals in three regions following increasing electrical currents (current, 0–1000 μA ; total stimulus duration, 1.0 s; pulse frequency, 20 Hz; pulse duration, 10 ms) in dark- and light-adapted conditions are shown as light reflectance changes. The peak values of light reflectance decrease during the 10-s recording period was used for the signal amplitude for each current (as in **C**). Note that the vertical scaling is different in the three recording regions (also in **C**). **C** Stimulus frequency and intrinsic signals. The intrinsic signals of three regions at increasing stimulus frequencies (pulse frequency, 5, 10, 15, 20, 40, 60, 80, and 100 Hz; total stimulus duration, 1.0 s; current, 500 μA) under dark-adapted conditions are shown as light reflectance changes. The results of five trials were averaged. Modified from Tsunoda et al., *Invest Ophthalmol Vis Sci.*³⁵ with permission.

visually evoked potentials,⁷¹ and electrically evoked pupillary reflexes,⁷⁵ which show maximal sensitivities, or responses, at a frequency of 15–20 Hz, have also been reported. The frequency-to-response curves in these studies are quite similar to those in our study.

The results of these studies indicate that electrical pulses applied transsclerally do not affect the photoreceptors, and that slow intrinsic signals evoked electrically reflect the activation of neurons in the inner and middle retinal layers. The similarity in the time course of the intrinsic signals elicited by both flash and electrical stimuli in these experiments indicates the possible contribution of stimulus-induced metabolic changes, such as blood flow and blood volume increases, following the activation of the inner or middle layers of the retina.

Experiment 3

This experiment was designed to determine whether slow intrinsic signals reflect the blood oxygenation level. Simultaneous measurements were obtained from the retina and primary visual cortex (V1) with observation lights of different wavelengths.

The origin of the intrinsic signals in the cerebral cortices has been extensively investigated, but most studies have dealt with the effects of the oxygenation levels of hemoglobin.^{21,76,77} The commonly accepted hypothesis is that the intrinsic signals in the cerebral cortex arise from light reflectance changes due to the many metabolic changes that occur following neural activation. For example, the intrinsic signal measured with a 570 nm observation light is domi-

nated by changes in the blood volume in the capillaries, at 600–650 nm it is dominated by changes in the oxygenation levels of hemoglobin, and in the infrared region it is dominated by changes in light scattering of the cortical tissues. Although the intrinsic signals measured by infrared light are thought to be free from changes in the oxygenation levels of hemoglobin,²⁷ some data indicate that the changes in the infrared light reflectance reflect the deoxygenation of hemoglobin in the cat retina.⁷⁸

The contribution of oxygenation levels of hemoglobin to the slow intrinsic signals was investigated by making simultaneous measurements from the retina and the primary visual cortex (V1) with different wavelengths of observation light. To measure the flash-evoked intrinsic signals in the cortex, a stainless steel chamber (17.0 mm in diameter) was mounted on the skull over the contralateral V1. The skull and the dura mater were removed within the chamber, and the chamber was filled with silicone oil (ADATOSIL-OL 1000, Bausch & Lomb, Heidelberg, Germany) and tightly sealed with a glass cover slip to reduce the movement of the cortex. The cortical surface was illuminated by two fiber optic light guides through the glass cover slip window, and the light reflectance was recorded with a CCD camera of the same type as for the retinal recordings.^{25,27} The entire imaged area was 8.8×6.6 mm imaged with 640×480 pixels. For the measurement of the signal intensity, we averaged the light reflectance changes in the central region, which covered 3.05×3.63 mm (222×264 pixels; Fig. 8A, right). The camera was focused 500 μ m below the cortical surface. The light from a halogen lamp was filtered through three band-pass filters, green (570 nm), red (630 nm), and infrared (870 nm). The flash luminance measured at the cornea was 56.1 cd/s/m².

The time courses of the intrinsic signals evoked by the three wavelengths of the observation light were compared at the optic disc and cortical area V1 (Fig. 8B and C). Although the absolute reflectance changes were different (Fig. 8C), the time course of the changes at the optic disc was the same for the three wavelengths (Fig. 8D): the reflectance slowly decreased following the flash, and reached its negative peak at the end of the recording period.³⁷ The time course of the intrinsic signals at V1, on the other hand, differed for the different wavelengths (Fig. 8C and D). The onset of the decrease in reflectance was the earliest with 630 nm, followed by 870 nm, and then by 570 nm. With 630 nm, the light reflectance change reached

a negative peak 2 s after the flash, and this was followed by an increase in the light reflectance that overshot the baseline reflectance. With 540 nm, the light reflectance changes reached a negative peak at 4.5 s, and with 870 nm, 3.0 s after the flash, but no large overshoot was observed. These time courses are almost the same as those with a grating stimulus.^{27,79}

Observation light at a wavelength of 570 nm can best determine the changes in blood volume, that at 630 nm those in deoxygenated hemoglobin, and that at 870 nm those in tissue light scattering. The reflectance pattern at the optic disc was the same for all wavelengths (Fig. 8D). This suggests that the change in blood oxygenation level is not the source of the slow signal observed at the optic disc, or that it is a negligibly small source compared with the contribution of the blood flow changes. It is generally assumed that the light scattering changes represent microscopic morphological changes elicited by neural activity, such as cell swelling associated with ion and water movements and changes in synaptic vesicle density associated with synaptic transmission. The light scattering changes are believed to be free of changes in blood volume or oxygenation, and the amplitudes are constant whichever wavelength is used for the observation light.²⁷ The amplitude of the signal at the optic disc, however, was almost four times larger at 570 nm than at either 630 nm or 870 nm. This is probably because the increase of the light scattering signal at the optic disc reflects the changes in the flow of red blood cells in the vessels, which are triggered by neural activity in the inner retina. It is well known that hemoglobin absorbs more green than red light. The ratio of blood-related light reflectance changes to the total tissue light reflectance changes can be much larger when illuminated at 570 nm than at either 630 nm or 870 nm. These observations are confirmed by the results of experiment 4.

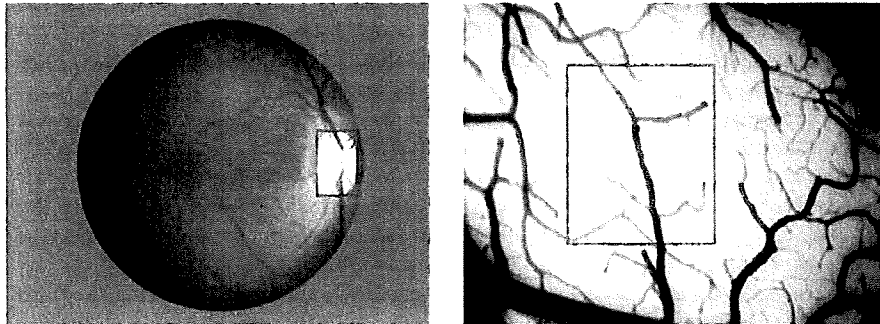
Experiment 4

This experiment was designed to determine the contribution of retinal blood flow to slow intrinsic signals. Flash-evoked retinal blood flow changes were measured by laser Doppler flowmetry.

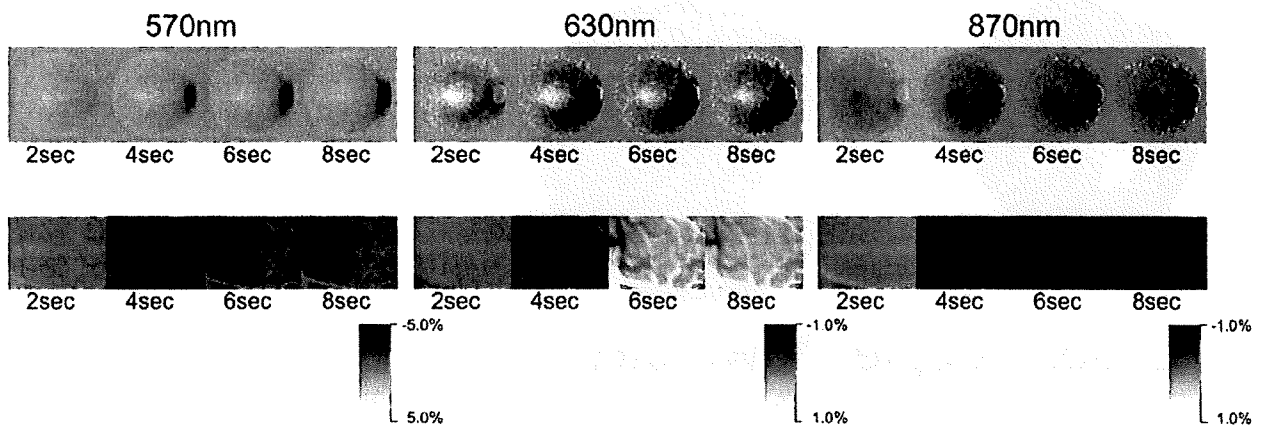
The flash-induced blood flow changes were measured by a laser Doppler flowmetry system (Perimed, Periflux 5010, Stockholm, Sweden; solid-state diode laser 780 μ m; power,

Figure 8A–D. Intrinsic signals recorded simultaneously from the optic disc and primary visual cortex (V1) with different wavelengths of observation light. **A** Images of the recorded regions in experiment 3: ocular fundus (*left*) and cortical area V1 (*right*). *Rectangles* indicate the areas used for data analyses. **B** Time courses of two-dimensional images of the ocular fundus (*top*) and cortical area V1 (*bottom*) showing the light reflectance changes evoked by flash stimulus recorded with different wavelengths of the observation light. Thirty consecutive video frames collected during 1 s were averaged for one poststimulus image. Darkened regions indicate a decrease of light reflectance following the flash stimulus. Note that the foveal regions observed at 570 and 630 nm become brighter following the flash due to the strong bleaching of the cone photopigments. **C** Plot of the time courses of flash-evoked light reflectance changes. The time following the flash is shown on the abscissa, and the delivery of the flash is indicated by the *arrowhead* (also in the following figures). Each point is the average of 15 video frames collected during 0.5 s of the light reflectance changes. The averages of ten trials are shown with the standard error of the means (SEMs). **D** Plot of the time courses of flash-evoked light reflectance changes, presented as relative values to the maximum in the optic disc and V1. Modified from Tsunoda et al., Invest Ophthalmol Vis Sci,³⁰ with permission.

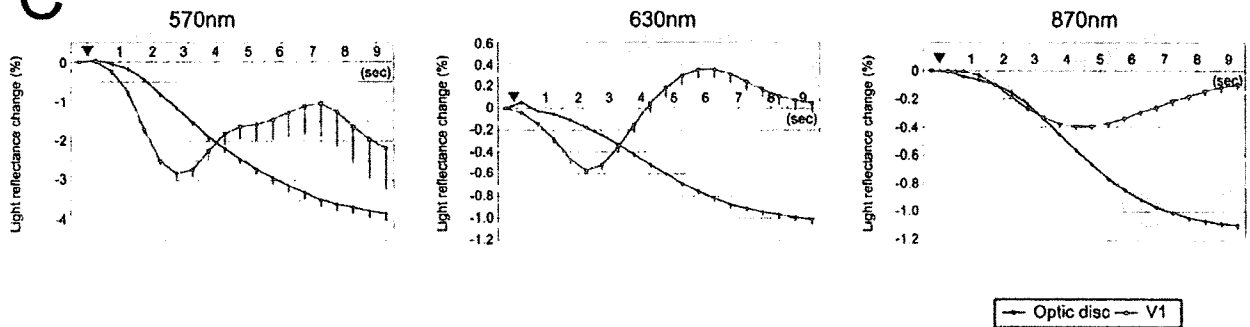
A



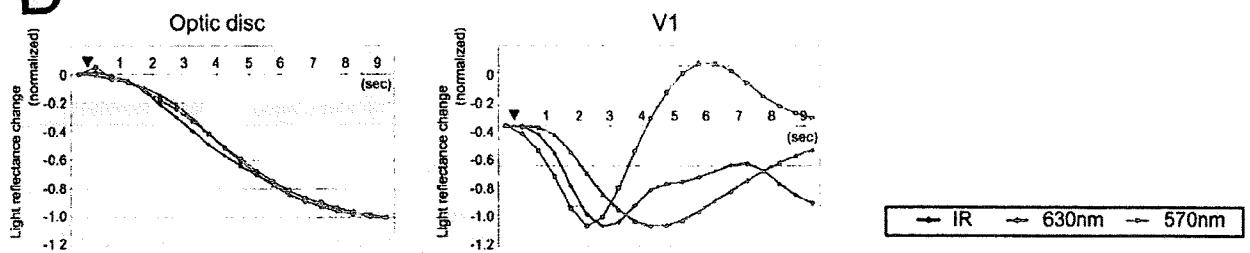
B



C



D



<1.0 mW; probe, PF403; probe diameter, 450 μ m; fiber separation, 250 μ m; time constant, 0.03) under aseptic conditions. Following a local peritomy of the conjunctiva, the laser probe was inserted through a scleral port, made at the 2 o'clock position 3.0 mm from the corneal limbus. The size of the sclerotomy was small enough to keep the intraocular pressure normal and constant during the recording. The laser probe was fixed firmly by a manual micromanipulator placed in front of the monkey's face. For the measurement of the blood flow changes at the optic disc and the posterior pole of the retina, the tip of the probe was placed <1.0 mm above these structures (Fig. 9A). The probe was pointed to a vessel-free region in order to measure averaged blood

flow changes in the capillaries. Blood flow is represented in arbitrary perfusion units (PU). The blood flow changes evoked by the flash stimulus were calculated by dividing the blood flow after the stimulus by the averaged blood flow during a 2.0-s period before the stimulus. The data of 20 consecutive trials were averaged.

The flash-induced blood flow changes of the ocular fundus were compared with the intrinsic signals evoked by the same flash intensity. The blood flow at the optic disc gradually increased and reached a peak 7.5 s following the flash (Fig. 9B). This time course was similar to that of the intrinsic signals (Fig. 9C). Similarly, the blood flow in the posterior retina gradually increased following the flash

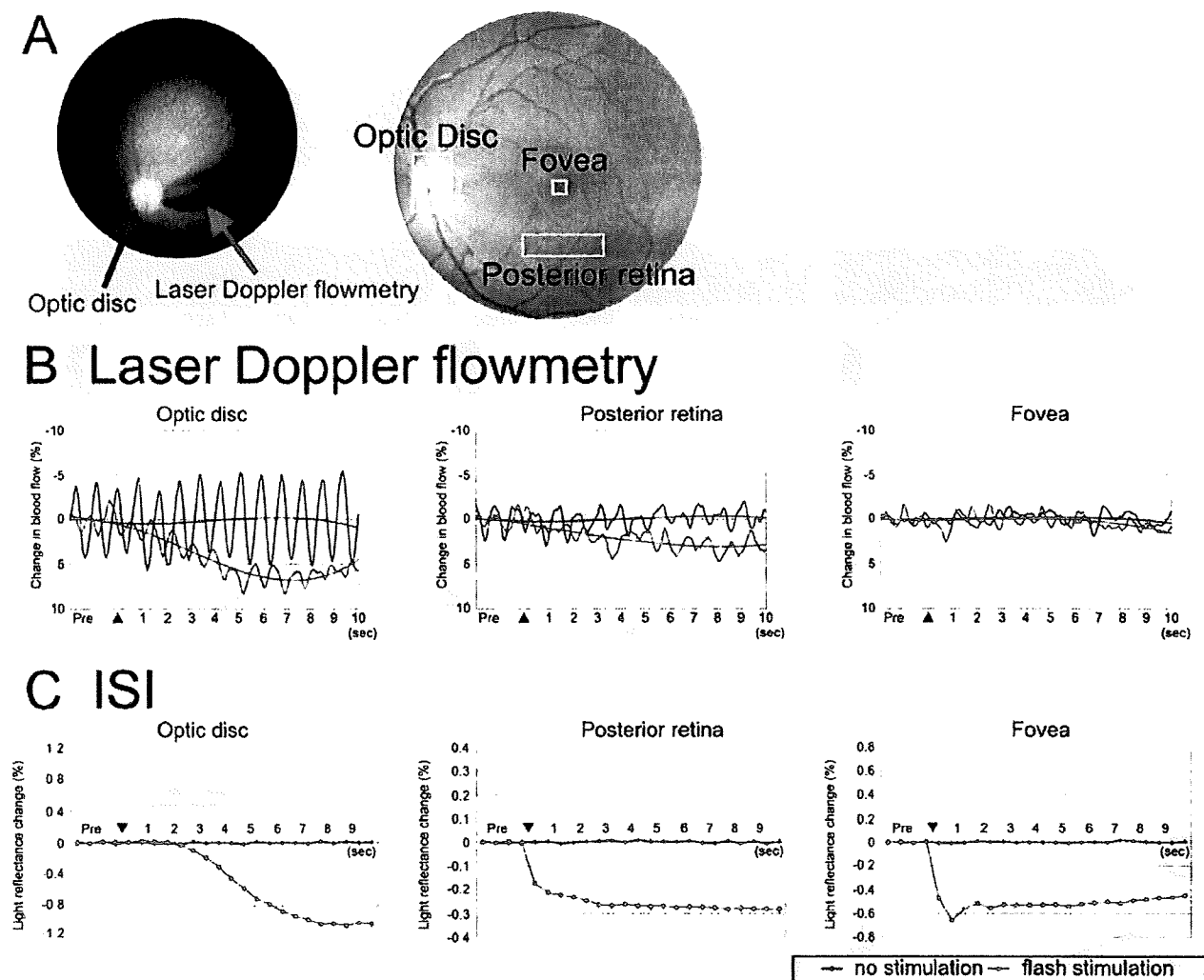


Figure 9A-C. Flash-induced blood flow changes of the ocular fundus measured by a laser Doppler flowmetry. **A** *Left:* measurement of blood flow at the optic disc by laser Doppler flowmetry. *Arrows* indicate the probe in the vitreous cavity and the location of the optic disc. *Right:* fundus photograph of normal retina showing the regions for the intrinsic signal imaging analysis in experiment 4. **B** Plot of the time courses of blood flow changes with (*red*) or without (*blue*) flashes, measured with laser Doppler flowmetry, from the three locations indicated in **A**. The averages of 20 trials is shown with polynomial trend lines (order 3). **C** Plot of the time courses of light reflectance changes with (*red*) or without (*blue*) flashes measured by the intrinsic signal imaging, from the three locations indicated in **A**. The averages of ten trials are shown with SEMs. Modified from Tsunoda et al., Invest Ophthalmol Vis Sci,³⁹ with permission.

and reached a peak at 8.0 s (Fig. 9B). This time course, however, was quite different from that of the intrinsic signal. The time course of the blood flow at the posterior retina did not have the same fast changes observed in the intrinsic signal imaging (Fig. 9C).

As shown in Fig. 3, the flash-evoked intrinsic signal in the posterior retina had two components: a fast light reflectance decrease that peaked at 100–200 ms (R_{fast} in Fig. 10C), and a slow light reflectance decrease that peaked at 6.0 s or later (R_{slow} in Fig. 10C).³⁷ The blood flow changes in the posterior retina appeared to match only the slow compo-

nent of the intrinsic signal imaging. In the foveal area, a flash-evoked blood flow change could not be observed by laser Doppler flowmetry, although large and fast light reflectance decreases were observed in the intrinsic signal imaging (Fig. 9B and C). Blood volume changes were also monitored using the same system, but no correlation between flash stimulus and blood volume changes could be observed in any recording region.

The results of experiment 4 show that the slow intrinsic signals at the optic disc and the posterior retina reflect blood flow increases following stimulation. The fast

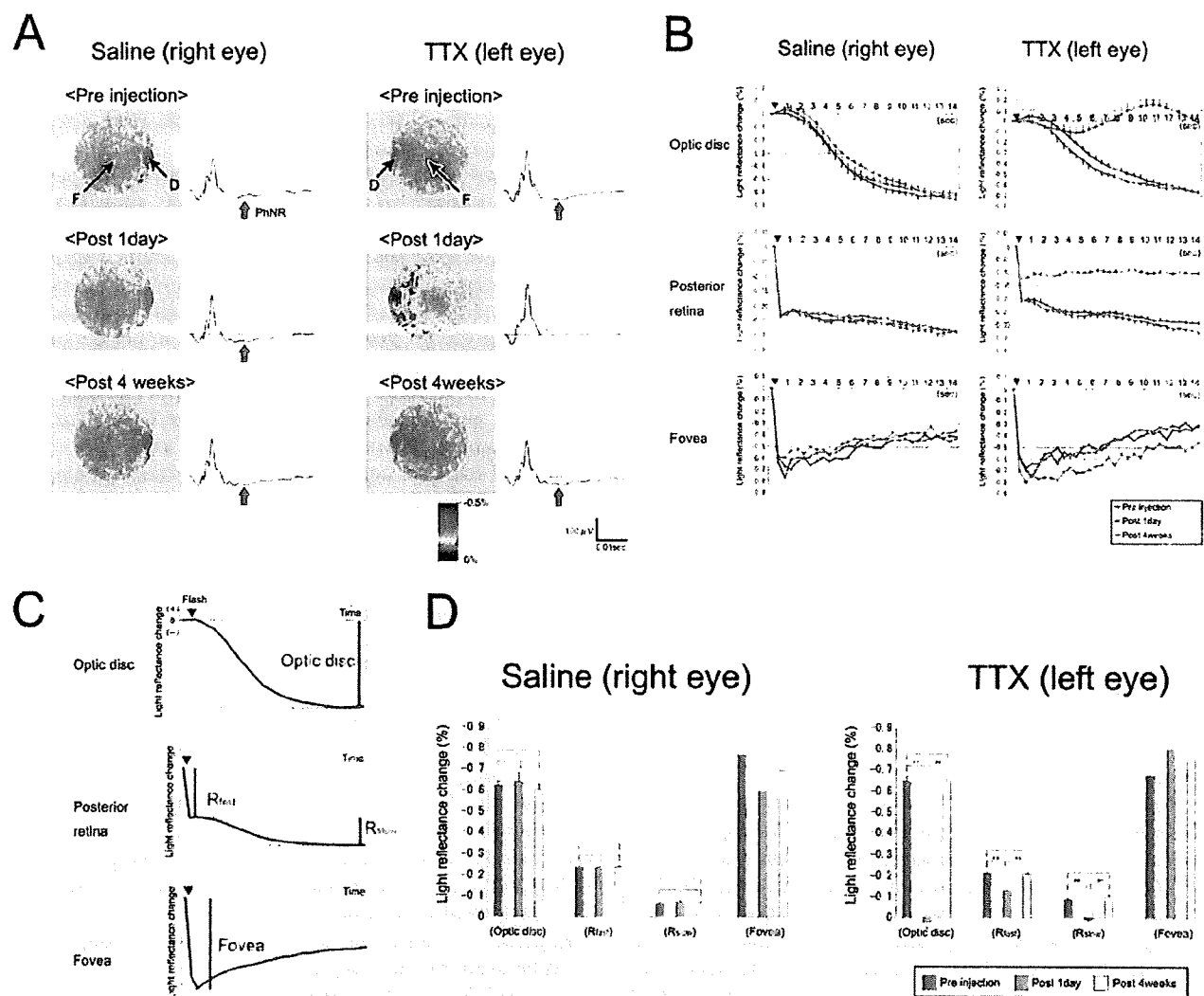


Figure 10A–C. Intrinsic signals of the ocular fundus before and after an intravitreal injection of tetrodotoxin (TTX). **A** Pseudocolor response topographic map of flash-evoked light reflectance changes with saline or TTX injection measured before the injection, 1 day after, and 4 weeks after. Each image was taken between 7 and 9 s following a flash. The ERG responses recorded on the same day are shown on the right. *Arrows* indicate the locations of optic disc (*D*) and fovea (*F*). *Red arrows* indicate the photopic negative response (*PhNR*). **B** Plot of the time courses of light reflectance changes with saline or TTX injection, measured from the three locations indicated in Fig. 9A. The results before the injection, 1 day after and 4 weeks after are shown by different colors. In the optic disc and posterior retina, the averages of 15 trials are shown with SEM. **C** Definition of the four components in flash-evoked intrinsic signals. **D** The changes in intrinsic signals following (*left*) saline and (*right*) TTX injections are shown for four signal components. $**P < 0.01$. Modified from Tsunoda et al., *Invest Ophthalmol Vis Sci*,³⁹ with permission.

changes observed in the intrinsic signal imaging at the fovea and the posterior retina could not be detected by laser Doppler flowmetry. Although the fast intrinsic signals were relatively large, they were independent of the blood flow changes. At the fovea, the blood flow changes measured by laser Doppler flowmetry are believed to reflect changes in the choroidal blood flow, caused by the lack of capillaries in the central 300 μm of the retina.⁸⁰ The blood flow in this region was constant even following a flash stimulus.

The trigger site of the blood flow increase following flash stimulus is still unclear. Riva et al.^{70,81} showed that the blood flow on the optic nerve head in both cats and humans increased following diffuse flicker stimulation when measured by laser Doppler flowmetry. Because the stimulus duration used in their studies was as long as 60 s, the precise time course of the signals immediately after the stimulus onset could not be determined. However, with extensive experiments, together with the data of patients with glaucoma, they concluded that the flash-evoked blood flow changes were induced by the activity of the retinal ganglion cells (RGCs).^{70,71,81,82}

Experiment 5

This experiment was designed to determine what triggers the blood flow increase following flash stimulation. The flash-induced intrinsic signals were recorded before and after an intravitreal injection of TTX.

To determine the cellular origins of the intrinsic signals, tetrodotoxin citrate (TTX; Wako Pure Chemical, Osaka, Japan) dissolved in physiological saline (50 μl , 8.0 μM) was injected into the vitreous cavity of one eye. Before the injection, 50 μl of the aqueous humor was removed from the anterior chamber with a 27 gauge needle. TTX was then injected through the pars plana (3.0 mm posterior to the corneal limbus) into the geometric center of the vitreous by a 27 gauge needle at the superior temporal position. The same amount of saline was injected by the same procedure into the vitreous cavity of the fellow eye for control recordings.

The slow intrinsic signals of the optic disc and the posterior retina are very sensitive (Fig. 4), and if a small region remains where the RGC function has not been completely blocked, a blood flow increase in the optic disc may be triggered by that region. It was therefore necessary to completely block the RGC responses over the whole retina. The intrinsic signals were also very susceptible to the physiological conditions of both the whole body and the eyeball, such as intraocular pressure, corneal curvature, and vitreous transparency. To obtain sufficient pharmacologic blockade and recovery of the physiological condition of the eye, the recording was not conducted on the day of injection. Intrinsic signal imaging and ERG recordings were made 1 week before the TTX injection, and 1 day and 4 weeks after the injection. In each recording session, the results of 15 recording trials, each of which had a 15-s recording time,

were averaged. To evoke the maximal response of the slow signal components, the recording trials were at intervals of 3 min (Fig. 6B).

To confirm the effect of TTX, the photopic negative response (PhNR)^{83,84} of the ERGs was recorded under light-adapted condition to evaluate the inner retinal activity on the same day as the intrinsic signal imaging measurements. A light-emitting diode (LED) contact lens electrode with background illumination source (Mayo) was placed on one eye. Following 15 min of light adaptation (background 25 cd/m^2), a white flash of 3.0 $\text{cd}/\text{s}/\text{m}^2$ intensity and 3 ms duration was emitted 15 times at 1.0-s interstimulus intervals. The ERGs were amplified $\times 10000$, and the band-pass filters were set at 0.3–500 Hz (Power Lab, ADInstruments). The PhNR was measured from the baseline to the first negative trough following the b wave in the cone ERG (Fig. 10A).^{83,84} Only the PhNR amplitude was reduced after the TTX injection, and it recovered to normal levels 4 weeks following the injection (Fig. 10A).

Pseudocolor maps of the signal distribution in the posterior pole averaged 7–9 s following flashes are shown in Fig. 10A. One day following the TTX injection, the intrinsic signals at the optic disc and the posterior retina, except in the foveal region, were reduced. The signal at the fovea did not change. Four weeks after the injection, the responses in the whole posterior pole were the same as before the injection. The time courses of the intrinsic signals both before and after TTX injection are shown in Fig. 10B. The response at the optic disc was abolished following the TTX injection. The fast component was partially reduced at the posterior retina, and the slow component was completely abolished by the TTX. The response at the fovea was not affected by the TTX injection.

The amplitudes of the four components of the intrinsic signals (optic disc, R_{fast} , R_{slow} , and fovea), for the 3 recording days were compared (Fig. 10C and D). Statistical analysis was performed with the Mann-Whitney *U* test to compare group means, and the differences were considered significant when $P < 0.05$. In the control eyes, there were no significant changes either in the optic disc or the posterior retina. In the eyes after TTX, the signals of optic disc and the R_{slow} component were abolished 1 day following the injection. The R_{fast} signals were significantly reduced 1 day following the injection (59.9% of the preinjection level). The intensity of the foveal response was not changed by the TTX injection, but the foveal responses could not be analyzed statistically because they required 30 min of dark adaptation, and only the initial trial following adaptation could be used for the comparison.

The RGCs are the major retinal elements that have spiking activity, and TTX can reduce their activity by blocking the Na^+ -dependent spikes.^{85,86} The PhNR is known to be reduced both in eyes with experimental glaucoma and after TTX injection, and thus is highly dependent on the spiking activity of inner retinal neurons.^{83,84} When one of the eyes in the present study was injected with TTX, the inner retinal activity was completely blocked. This suggests that the slow intrinsic signals observed at the posterior

retina and the optic disc represent the blood flow increases following flash-induced spiking activity in the inner retina. The foveal region used for this analysis contains no RGCs, so foveal signals were not affected by TTX. Amacrine cells are also known to produce spikes, but the proportion of amacrine cells that contribute to the intrinsic signal is not known. It must be noted that the slow intrinsic signals in the posterior retina and the optic disc do not represent only the activity of RGCs. Riva et al.⁷¹ have shown that in patients with ocular hypertension and early glaucoma, the blood flow increases at the optic disc following flickering flash stimulus are abnormally low. As RGCs rather than amacrine cells are the major neural elements affected by these disorders,⁸⁷⁻⁹² it is reasonable that the reduction of RGC activity in the posterior pole can be detected by intrinsic signal imaging.

Questions Still to Be Answered for Understanding the Origin of Intrinsic Signals in the Retina

The part of the fast intrinsic signals of the posterior retina that was not affected by TTX (R_{fast} in Fig. 10D) must originate from the activity of neurons more distal than the RGCs. The amplitude of the R_{fast} signal (R1 in Fig. 6) did not decrease with shorter interstimulus intervals, but attained a maximum with 3-min intervals equal to the D and R2 signals. This suggests that the R_{fast} component reflects changes in both inner and outer retinal activities. The cellular origin of the non-blood-related fast light scattering signals, however, may not be easily solved because each type of neural cell, such as photoreceptors, bipolar cells, and Müller cells, may have its own independent characteristics in producing reflectance changes following neural activation.

Focally stimulated regions show a decrease in light reflectance following the stimulus, and this darkened region matches the location of the focal stimulus exactly (Fig. 1C). What is striking is that the nonstimulated regions show slow light reflectance increases,³⁷ which cannot be easily explained by the results of experiments 1 to 5. The brightening observed in the nonstimulated regions in the later phases might be explained by (1) horizontal interaction by, for example, horizontal cells through which stimulated neurons could affect the reflectivity of the neurons outside the stimulated region; (2) a periphery/shift effect, in which a large stimulus remote from the center of the receptive field of RGCs can alter the responsiveness of the RGCs⁹³⁻⁹⁵; and (3) spatial interaction of the intrinsic signals between the stimulated and nonstimulated regions by an inhomogeneous distribution of capillary blood flow.^{21,76,77,96} These explanations, however, do not account for the strong and homogeneous brightening over the whole posterior region triggered by a small focal stimulus.⁹⁷ It is possible that the properties of the intrinsic signals, such as polarity and threshold, are different in different retinal layers, and different layers are dominantly activated in stimulated and nonstimulated regions.^{98,99}

Recent in vivo functional OCT (fOCT) showed that the properties of the flash-evoked light scattering changes were different in the outer and inner segments of the photoreceptors.^{46,100} We have recently built a spectral domain-OCT system, by which both functional OCT and intrinsic signals can be measured from the macaque's retina through the same optical pathway. Preliminary results show that not only the fast functional OCT signals in the outer segment layer but also slow signals in the RGC and nerve fiber layers can be observed. The time course in the RGC layer matches that of the slow intrinsic signals at the optic disc exactly. Thus, fOCT may be a valuable technique to resolve the problems relating to the origins of retinal intrinsic signals.

Conclusions

The present experiments on the intrinsic signals from the macaque's retina revealed that:

1. Four different types of signals can be evoked by a bright flash stimulus in the posterior retina: a fast signal at the fovea, fast and slow signals at the posterior retina, and a slow signal at the optic disc.
2. The fast signals at the fovea and the posterior retina are derived from light scattering changes in the photoreceptor layer and are not related to changes in the blood flow or blood oxygenation levels in the retina or choroid. These light scattering changes are thought to be derived from structural changes in the outer segment disks, membrane hyperpolarization, cell swelling, and changes in the composition of the interphotoreceptor matrix.
3. The slow signals at the posterior pole and the optic disc are very sensitive to light stimuli, and their thresholds are comparable to those of the ERG b wave in the dark-adapted condition. Slow signals are independent of the changes in the blood oxygenation level, and derive from blood flow increases in the vessels and capillaries. RGCs are major triggers of these flow changes. These slow signals are also evoked by transscleral electrical stimulation.
4. The amplitudes of the slow signals are largest at 3- to 5-min interflash intervals, and decrease at both shorter and longer interflash intervals, indicating a neurovascular interaction in the inner retina, in which blood flow can be increased with repetitive stimuli.
5. There seem to be other signal components whose origins cannot be explained by these experiments.

The complex properties of the retinal intrinsic signals indicate that the flash-evoked signals reflect a combination of light reflectance changes occurring independently and concurrently in the different retinal layers from the photoreceptor layer to the RGC layer. Functional OCT measurements are expected to be a valuable tool for investigating the still unsolved problems relating to the origin of the retinal intrinsic signals.

References

1. Webb RH, Hughes GW. Scanning laser ophthalmoscope. *IEEE Trans Biomed Eng* 1981;28:488–492.
2. Mainster MA, Timberlake GT, Webb RH, Hughes GW. Scanning laser ophthalmoscopy. Clinical applications. *Ophthalmology* 1982;89:852–857.
3. Huang D, Swanson EA, Lin CP, et al. Optical coherence tomography. *Science* 1991;254:1178–1181.
4. Hee MR, Izatt JA, Swanson EA, et al. Optical coherence tomography of the human retina. *Arch Ophthalmol* 1995;113:325–332.
5. Rushton WA. The difference spectrum and the photosensitivity of rhodopsin in the living human eye. *J Physiol* 1956;134:11–29.
6. Hood C, Rushton WA. The Florida retinal densitometer. *J Physiol* 1971;217:213–229.
7. Rushton WA. Cone pigment kinetics in the protanope. *J Physiol* 1963;168:374–388.
8. Alpern M, Maasoidvaag F, Oba N. The kinetics of cone visual pigments in man. *Vision Res* 1971;11:539–549.
9. Alpern M. Rhodopsin kinetics in the human eye. *J Physiol* 1971;217:447–471.
10. van Norren D, van de Kraats J. Retinal densitometer with the size of a fundus camera. *Vision Res* 1989;29:369–374.
11. Kilbride PE, Read JS, Fishman GA, Fishman M. Determination of human cone pigment density difference spectra in spatially resolved regions of the fovea. *Vision Res* 1983;23:1341–1350.
12. Kilbride PE, Keehan KM. Visual pigments in the human macula assessed by imaging fundus reflectometry. *Appl Opt* 1990;29:1427–1435.
13. Faulkner DJ, Kemp CM. Human rhodopsin measurement using a T.V.-based imaging fundus reflectometer. *Vision Res* 1984;24:221–231.
14. Kemp CM, Faulkner DJ, Jacobson SG. The distribution and kinetics of visual pigments in the cat retina. *Invest Ophthalmol Vis Sci* 1988;29:1056–1065.
15. Kemp CM, Jacobson SG, Faulkner DJ. Two types of visual dysfunction in autosomal dominant retinitis pigmentosa. *Invest Ophthalmol Vis Sci* 1988;29:1235–1241.
16. van Norren D, van de Kraats J. Imaging retinal densitometry with a confocal scanning laser ophthalmoscope. *Vis Res* 1989;29:1825–1830.
17. Elsner AE, Burns SA, Hughes GW, Webb RH. Reflectometry with a scanning laser ophthalmoscope. *Appl Opt* 1992;31:3697–3710.
18. Elsner AE, Burns SA, Beausencourt E, Weiter JJ. Foveal cone photopigment distribution: small alterations associated with macular pigment distribution. *Invest Ophthalmol Vis Sci* 1998;39:2394–2404.
19. Zepeda A, Arias C, Sengpiel F. Optical imaging of intrinsic signals: recent developments in the methodology and its applications. *J Neurosci Methods* 2004;136:1–21.
20. Ts'o DY, Frostig RD, Lieke EE, Grinvald A. Functional organization of primate visual cortex revealed by high resolution optical imaging. *Science* 1990;249:417–420.
21. Frostig RD, Lieke EE, Ts'o DY, Grinvald A. Cortical functional architecture and local coupling between neuronal activity and the microcirculation revealed by in vivo high-resolution optical imaging of intrinsic signals. *Proc Natl Acad Sci U S A* 1990;87:6082–6086.
22. Roe AW, Ts'o DY. Visual topography in primate V2: multiple representation across functional stripes. *J Neurosci* 1995;15:3689–3715.
23. Ghose GM, Ts'o DY. Form processing modules in primate area V4. *J Neurophysiol* 1997;77:2191–2196.
24. Malonek D, Tootell RB, Grinvald A. Optical imaging reveals the functional architecture of neurons processing shape and motion in owl monkey area MT. *Proc R Soc Lond B Biol Sci* 1994;258:109–119.
25. Tsunoda K, Yamane Y, Nishizaki M, Tanifuji M. Complex objects are represented in macaque inferotemporal cortex by the combination of feature columns. *Nat Neurosci* 2001;4:832–838.
26. MacVicar BA, Hochman D. Imaging of synaptically evoked intrinsic optical signals in hippocampal slices. *J Neurosci* 1991;11:1458–1469.
27. Bonhoeffer T, Grinvald A. Optical imaging based on intrinsic signals: the methodology. In: Toga AW, Mazziotta JC, editors. *Brain mapping*. San Diego: Academic Press; 1996. p. 55–97.
28. Weliky M, Kandler K, Fitzpatrick D, Katz LC. Patterns of excitation and inhibition evoked by horizontal connections in visual cortex share a common relationship to orientation columns. *Neuron* 1995;15:541–552.
29. Das A, Gilbert CD. Long-range horizontal connections and their role in cortical reorganization revealed by optical recording of cat primary visual cortex. *Nature* 1995;375:780–784.
30. Tsunoda K, Oguchi Y, Hanazono G, Tanifuji M. Mapping cone- and rod-induced retinal responsiveness in macaque retina by optical imaging. *Invest Ophthalmol Vis Sci* 2004;45:3820–3826.
31. Crittin M, Riva CE. Functional imaging of the human papilla and peripapillary region based on flicker-induced reflectance changes. *Neurosci Lett* 2004;360:141–144.
32. Abramoff MD, Kwon YH, Ts'o D, et al. Visual stimulus-induced changes in human near-infrared fundus reflectance. *Invest Ophthalmol Vis Sci* 2006;47:715–721.
33. Grieve K, Roorda A. Intrinsic signals from human cone photoreceptors. *Invest Ophthalmol Vis Sci* 2008;49:713–719.
34. Nelson DA, Krupsky S, Pollack A, et al. Special report: noninvasive multi-parameter functional optical imaging of the eye. *Ophthalmic Surg Lasers Imaging* 2005;36:57–66.
35. Harary HH, Brown JE, Pinto LH. Rapid light-induced changes in near infrared transmission of rods in *Bufo marinus*. *Science* 1978;202:1083–1085.
36. Yao XC, Yamauchi A, Perry B, George JS. Rapid optical coherence tomography and recording functional scattering changes from activated frog retina. *Appl Opt* 2005;44:2019–2023.
37. Hanazono G, Tsunoda K, Shinoda K, Tsubota K, Miyake Y, Tanifuji M. Intrinsic signal imaging in macaque retina reveals different types of flash-induced light reflectance changes of different origins. *Invest Ophthalmol Vis Sci* 2007;48:2903–2912.
38. Inomata K, Tsunoda K, Hanazono G, et al. Distribution of retinal responses evoked by transscleral electrical stimulation detected by intrinsic signal imaging in macaque monkeys. *Invest Ophthalmol Vis Sci* 2008;49:2193–2200.
39. Hanazono G, Tsunoda K, Kazato Y, Tsubota K, Tanifuji M. Evaluating neural activity of retinal ganglion cells by flash-evoked intrinsic signal imaging in macaque retina. *Invest Ophthalmol Vis Sci* 2008;49:4655–4663.
40. Wali N, Leguire LE. The photopic hill: a new phenomenon of the light adapted electroretinogram. *Doc Ophthalmol* 1992;80:335–345.
41. Wagman IH, Waldman J, Naidoff D, Feinschil LB, Cahan R. The recording of the electroretinogram in humans and in animals; investigation of retinal sensitivity following brief flashes of light. *Am J Ophthalmol* 1954;38:60–69.
42. Mahroo OA, Lamb TD. Recovery of the human photopic electroretinogram after bleaching exposures: estimation of pigment regeneration kinetics. *J Physiol* 2004;554:417–437.
43. Weinhaus RS, Burke JM, Delori FC, Snodderly DM. Comparison of fluorescein angiography with microvascular anatomy of macaque retinas. *Exp Eye Res* 1995;61:1–16.
44. Roy C, Sherrington C. On the regulation of the blood supply of the brain. *J Physiol* 1890;11:85–108.
45. Villringer A, Dirnagl U. Coupling of brain activity and cerebral blood flow: basis of functional neuroimaging. *Cerebrovasc Brain Metab Rev* 1995;7:240–276.
46. Bizheva K, Pflug R, Hermann B, et al. Optophysiology: depth-resolved probing of retinal physiology with functional ultrahigh-resolution optical coherence tomography. *Proc Natl Acad Sci U S A* 2006;103:5066–5071.